12. Gubbay, J. *et al.* A gene mapping to the sex-determining region of the mouse Y chromosome is a member of a novel family of embryonically expressed genes. *Nature* **346,** 245–250 (1990).
13. Eicher, E. M., Washburn, L. L., Whitney, J. B. III & Morrow, K. E. *Mus poschiavinus* Y chromosome in the C57BL/6J murine genome causes sex reversal. *Science* **217,** 535–537 (1982).
14. Eicher, E. M. & Washburn, L. L. Inherited sex reversal in mice: identification of a new primary sex-determining gene. *J. Exp. Zool.* **228,** 297–304 (1983).
15. Nagamine, C. M. *et al.* The musculus-type Y chromosome of the laboratory mouse is of Asian origin. *Mamm. Genome* **3,** 84–91 (1992).
16. Luo, X., Ikeda, Y. & Parker, K. L. A cell-specific nuclear receptor is essential for adrenal and gonadal development and sexual differentiation. *Cell* **77,** 481–490 (1994).
17. Wagner, T. *et al.* Autosomal sex reversal and campomelic dysplasia are caused by mutations in and around the SRY-related gene SOX9. *Cell* **79,** 1111–1120 (1994).
18. Foster, J. W. *et al.* Campomelic dysplasia and autosomal sex reversal caused by mutations in an *SRY*-related gene. *Nature* **372,** 525–530 (1994).
19. Uchida, K. *et al.* Exclusion of *Sox9* as a candidate for the mouse mutant Tail-short. *Mamm. Genome* **7,** 481–485 (1996).
20. Coré, N. *et al.* Altered cellular proliferation and mesoderm patterning in Polycomb-M33-deficient mice. *Development* **124,** 721–729 (1997).
21. Kessel, M., Balling, R. & Gruss, P. Variation of cervical vertebrae after expression of a *Hox-1.1* transgene in mice. *Cell* **61,** 301–308 (1990).
22. Takihara, Y. *et al.* Targeted disruption of the mouse homologue of the *Drosophila* polyhomeotic gene lead to altered anteroposterior patterning and neural crest defects. *Development* **124,** 3673–3682 (1997).
23. van der Lugt, N. M. T. *et al.* Posterior transformation, neurological abnormalities, and severe hematopoietic defects in mice with a targeted deletion of the *bmi-1* proto-oncogene. *Genes Dev.* **8,** 757–769 (1994).
24. Akasaka, T. *et al.* A role for mel-18, a Polycomb group-related vertebrate gene, during the anteroposterior specification of the axial skeleton. *Development* **122,** 1513–1522 (1996).
25. Mittwoch, U. Sex differentiation in mammals and tempo of growth probabilities vs. switches. *J. Theor. Biol.* **137,** 445–455 (1989).
26. Cattanach, B. M. Sex-reversed mice and sex determination. *Ann. N. Y. Acad. Sci.* **513,** 27–39 (1987).
27. Burgoyne, P. S. & Palmer, S. J. The genetics of XY sex reversal in the mouse and other mammals. *Semin. Dev. Biol.* **2,** 277–284 (1991).
28. Bunker, C. A. & Kingston, R. E. Transcription repression by *Drosophila* and Mammalian Polycomb group proteins in transfected mammalian cells. *Mol. Cell. Biol.* **14,** 1721–1732 (1994).
29. Boer, P. H. *et al.* Polymorphisms in the coding and noncoding regions of murine *Pgk*-1 alleles. *Biochem. Genet.* **28,** 299–308 (1990).
30. Robertson, E. J. in *Teratocarcinomas and Embryonic Stem Cells: A Practical Approach* (ed. Robertson, E. J.) 71–112 (IRL, Oxford, 1987).

Acknowledgements. We thank T. Takeuchi, Y. Takihara, H. Koseki and T. Akasaka for advice and discussion; M. Djabali for communicating unpublished results; and R. A. Shiurba for critical reading of the manuscript.

Correspondence and requests for materials should be addressed to Y.K.-F. (e-mail: kan@libra.ls.m-kagaku.co.jp).

Premotor commands encode monocular eye movements

Wu Zhou & W. M. King

University of Mississippi Medical Center, Departments of Neurology and Anatomy, 2500 North State Street, Jackson, Mississippi 39216, USA

Binocular coordination of eye movements is essential for stereopsis (depth perception) and to prevent double vision. More than a century ago, Hering and Helmholtz debated the neural basis of binocular coordination. Helmholtz[1] believed that each eye is controlled independently and that binocular coordination is learned. Hering[2] believed that both eyes are innervated by common command signals that yoke the eye movements (Hering's law of equal innervation). Here we provide evidence that Hering's law is unlikely to be correct. We show that premotor neurons in the paramedian pontine reticular formation that were thought to encode conjugate[3–6] velocity commands for saccades (rapid eye movements) actually encode monocular commands for either right or left eye saccades. However, 66% of the abducens motor neurons, which innervate the ipsilateral lateral rectus muscle, fire as a result of movements of either eye. The distribution of sensitivity to ipsilateral and contralateral eye movements across the abducens motor neuron pool may provide a basis for learning binocular coordination in infancy and adapting it throughout life.

Abducens motor neurons are the final common pathway along which neural commands travel to innervate the lateral rectus muscle of the eye unilaterally. Figure 1 illustrates the discharge pattern of an abducens motor neuron located on the right side during 'smooth pursuit' movements in which only one eye moved; we name these movements 'monocular pursuit' movements. Firing rate decreased when the ipsilateral eye adducted and increased when it abducted (Fig. 1a, thin trace). This is the expected discharge pattern of an abducens motor neuron[7]. Unexpectedly, however, during monocular pursuit movements of the contralateral eye (Fig. 1b, thick trace), the cell's firing rate was also modulated even though the ipsilateral eye was stationary. To examine this relationship quantitatively, we calculated mean eye position and firing rate over 50-ms intervals (Fig. 1c, d). Firing rate is linearly related to ipsilateral (Fig. 1c, black circles) and contralateral (Fig. 1d, open triangles) eye position. The regression coefficient relating firing rate to ipsilateral eye position (3.3 spikes s^{-1} deg^{-1}) is greater than the coefficient relating firing rate to contralateral eye position (2.3 spikes s^{-1} deg^{-1}). Not every abducens motor neuron exhibits binocular discharge characteristics. Figure 2 illustrates the activity of a motor neuron with a monocular discharge pattern: its firing rate is related to ipsilateral eye position (Fig. 2a, c, 4.1 spikes s^{-1} deg^{-1}, $P < 0.001$) but not to contralateral eye position (Fig. 2b, d, 0.002 spikes s^{-1} deg^{-1}, $P > 0.97$).

To determine the distribution of sensitivity to ipsilateral and contralateral eye movements across the motor neuron pool, we obtained single unit recordings from 136 motor neuron axons. Multiple regression analyses showed that many motor neurons were monocular, with regression coefficients relating firing

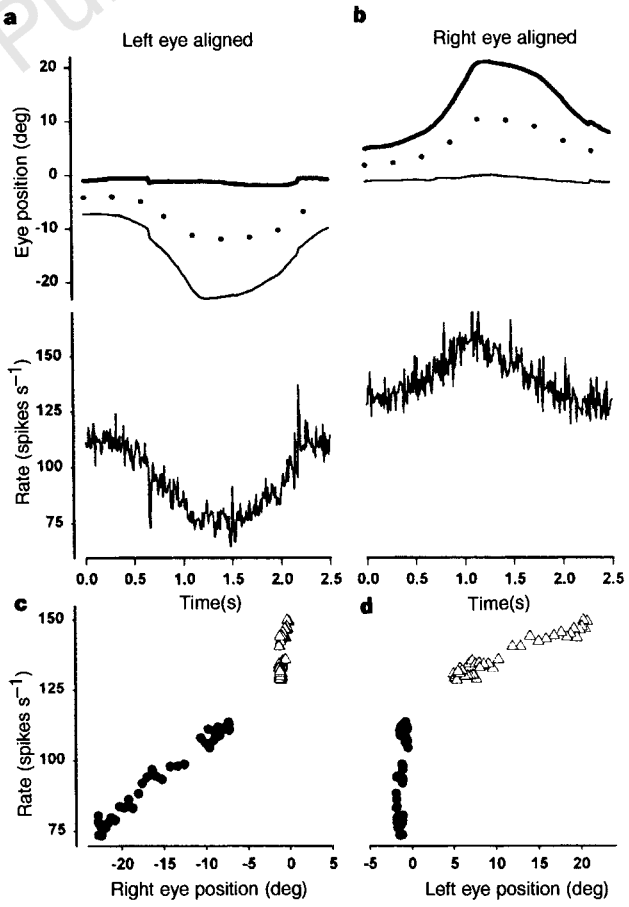

Figure 1 Discharge pattern of a binocular abducens motor neuron recorded in the VIth nerve. **a**, Monocular pursuit, aligned with the monkey's left eye, of a visible target that is moved towards or away from the animal in a sagittal plane. Upper panel, the left eye (thick trace) is relatively stationary while the right eye (thin trace) tracks the target. Eye movement to the left is indicated by downward deflection of the traces, and movement to the right is indicated by an upward trace deflection (in Figs 1, 2 and 4). The dotted trace indicates the conjugate eye position. Lower panel, rate of firing of abducens motor neurons. **b**, Monocular pursuit aligned with the right eye. **c**, **d**, Firing rate correlates linearly with right eye position (**c**, black circles) and left eye position (**d**, open triangles).

rate either to ipsilateral (Fig. 3a, black circles) or to contralateral (Fig. 3a, black triangles) eye position ($P < 0.05$). The mean sensitivity of monocular motor neurons to eye position was 3.84 ± 1.03 spikes s^{-1} deg^{-1} ($N = 37$) for ipsilateral eye units and 2.72 ± 1.48 spikes s^{-1} deg^{-1} ($N = 9$) for contralateral eye units. We only classified cells as monocular if one of the regression coefficients was not significantly different from zero ($P > 0.05$, 32 out of 46 cells) or if the regression, R^2, was unchanged by including the smaller coefficient ($P > 0.05$, 14 out of 46 cells). The remaining 90 motor neurons were binocular, with significant regression coefficients for the ipsilateral (3.39 ± 1.19 spikes s^{-1} deg^{-1}, grey circles) and contralateral (1.40 ± 0.63 spikes s^{-1} deg^{-1}, grey triangles) eye.

The distribution of regression coefficients is not uniform (Fig. 3a, upper panel). To illustrate this effect, we calculated a numerical index called ocular selectivity (Fig. 3a, lower panel). Monocular motor neurons have ocular selectivities clustered at either end of the distribution (Fig. 3a, lower panel, black bars). Of these monocular motor neurons, 27% are monocular with respect to the ipsilateral eye (mean ocular selectivity = 0.86, s.d. = 0.09) and 7% are monocular with respect to the contralateral eye (mean = −0.94, s.d. = 0.06). Ocular selectivities of binocular motor neurons are distributed in between (66%, grey bars), with a clear preference for the ipsilateral eye ($0 <$ ocular selectivity < 1, mean = 0.34, s.d. = 0.31).

As left or right eye position is a linear sum of conjugate and vergence eye positions, these data do not resolve the conflict between Hering's and Helmholtz's hypotheses. For example, cells

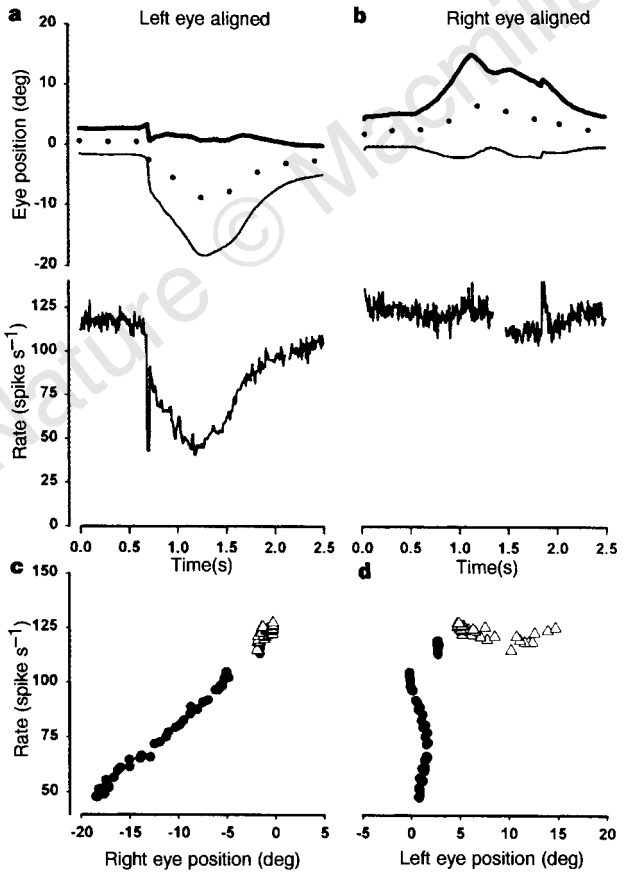

Figure 2 Discharge pattern of a monocular abducens motor neuron. **a**, Monocular pursuit with the ipsilateral eye (right eye, thin trace). **b**, Monocular pursuit with the left eye (thick trace). **c**, **d**, Firing rate correlates linearly with right eye position (**c**) but not with left eye position (**d**). Black circles represent data from trials in **a** (left eye aligned), and open triangles represent data from trials in **b** (right eye aligned).

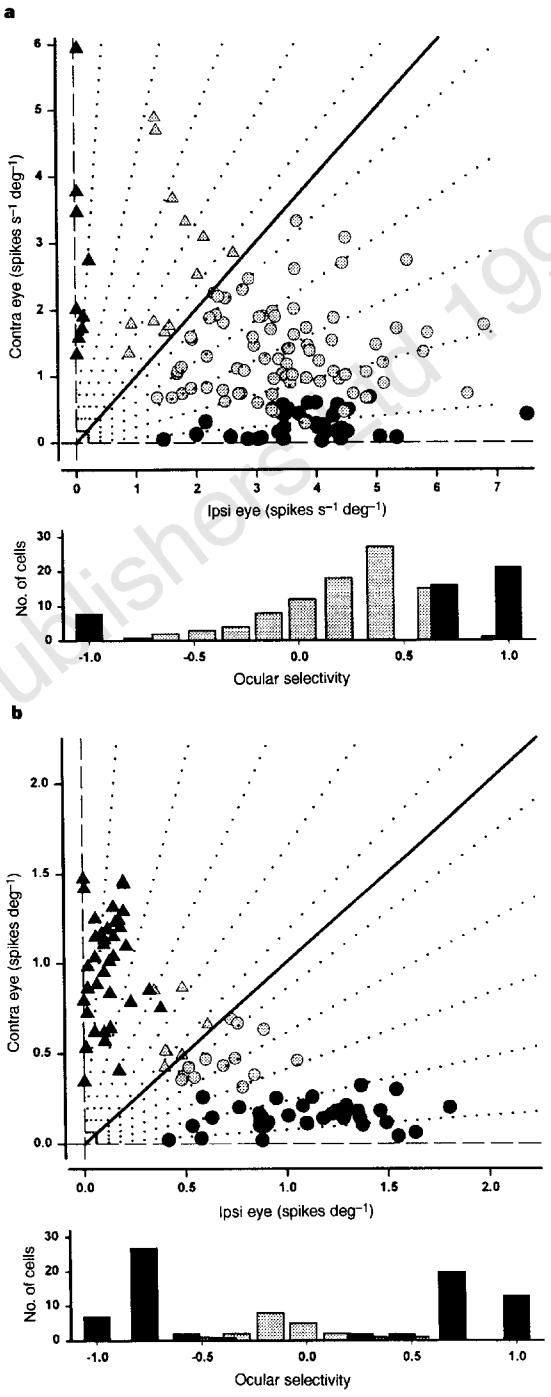

Figure 3 The distribution of regression coefficients relating neuronal discharge to contralateral or ipsilateral eye position or saccade amplitude. **a**, Upper panel, regression coefficients for abducens motor neurons. Black symbols represent monocular motor neurons; grey symbols represent binocular units. Circles represent cells with ipsilateral (ipsi) eye preference, and triangles represent cells with contralateral (contra) eye preference. Lower panel, distribution of ocular selectivity. Black bars correspond to monocular motor neurons, and grey bars correspond to binocular motor neurons. **b**, Regression coefficients (upper panel) and ocular selectivity (lower panel) for EBNs. Symbols as in **a**. Note the expanded scale in the upper panel. In each upper panel, the dotted lines define 9-degree wedges centred about the axes and about the unity slope line (thick black line). These wedges define the bins used in the ocular selectivity plots. Ocular selectivity for motor neurons is defined as $(K_{ipsi} - K_{contra})/(K_{contra} + K_{ipsi})$, where K_{contra} and K_{ipsi} are the regression coefficients relating firing rate to contralateral or ipsilateral eye position, respectively. For EBNs, ocular selectivity is defined similarly except the regression coefficients relate the number of spikes for saccade amplitude. Ocular selectivity is >0 for ipsilateral eye preference.

that we have classified as monocular might simply receive balanced conjugate and vergence input signals that cancel one another out during monocular pursuit[8]. To distinguish between these hypotheses one can record the activity of premotor cells during disjunctive eye movements that strongly dissociate right and left eye position. Excitatory burst neurons (EBNs) in the paramedian pontine reticular formation (PPRF) project directly to motor neurons[9]. During saccades, EBNs discharge a burst of spikes that encodes eye velocity. The burst is integrated by a neuronal circuit involving nucleus prepositus hypoglossi (NPH) neurons to produce an eye-position command[9]. Thus the number of spikes in the burst is correlated with the amplitude of the saccade[10]. For example, during ipsilateral conjugate eye movements of 10 degrees, the EBN shown in Fig. 4a emitted bursts of 8–11 spikes. During monocular 10-degree saccades executed by the right eye (Fig. 4b), the EBN continued to emit bursts of 8–10 spikes despite the reduction of conjugate saccade amplitude (Fig. 4b, grey traces) to 5 degrees in these trials. This cell never discharged during conjugate saccades to the contralateral side. However, during asymmetric vergence saccades with contralateral conjugate components (Fig. 4c), the cell emitted bursts of 4–7 spikes, consistent with the ipsilateral saccade of 3–5 degrees made by the right eye. These data indicate that this cell monocularly encodes movements of the right eye. Indeed, multiple regression analysis of data from many trials shows that the number of spikes in a burst encodes the amplitude of right eye saccades (Fig. 5a; -1.00 ± 0.05 spikes deg^{-1}, $P < 0.001$) but not the amplitude of left eye saccades (Fig. 5b; 0.02 ± 0.04 spikes deg^{-1}, $P > 0.55$).

In Fig. 5c, d, we show similar data from another EBN but include divergence as well as convergence trials. Data from divergence trials (black triangles) overlay data from convergence (grey inverted triangles) and conjugate (grey circles) saccade trials when plotted against the amplitude of the left eye saccade. This EBN encoded the amplitude of the left eye saccade (Fig. 5c; 1.29 ± 0.04 spikes deg^{-1}, $P < 0.001$) but not of the right eye saccade (Fig. 5d; -0.06 ± 0.04 spikes deg^{-1}, $P > 0.11$). In Fig. 3b we show that most of the 96 studied EBNs were monocular (79%, black symbols). Only 5.3% (five cells) clustered near the unity slope line could be said to encode conjugate saccade amplitude.

We further tested each of the EBNs that we classified as monocular for any possible relationship to conjugate saccade amplitude. We selected a subset of trials for which the amplitude of the saccades made by the eye associated with the larger regression coefficient was constant, while the other eye executed saccades of varying amplitude (thus conjugate amplitude varied over a large range). For each neuron, we calculated the regression of the number of spikes related to conjugate saccade amplitude; in every case, the regression was not significant ($P > 0.05$). Furthermore, for every monocular neuron, the correlation coefficient, R, of the monocular regression (amplitude of the ipsilateral or contralateral eye saccade) was significantly greater than the regression for conjugate amplitude ($P < 0.05$).

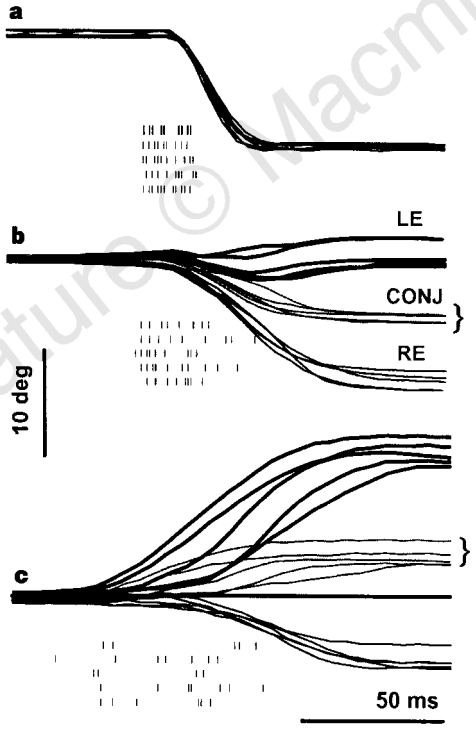

Figure 4 Excitatory burst neurons in the left PPRF encode monocular eye movements. **a**, Leftward conjugate saccades of 10 degrees. **b**, Monocular saccades of 10 degrees in the right eye. **c**, Convergent saccades of about 10 degrees. The thick traces indicate left eye (LE) position; the bracketed traces indicate conjugate position (CONJ); and the thin traces indicate right eye (RE) position. Each record consists of five superimposed trials. Neural action potentials are represented as vertical tick marks aligned with the eye movement records.

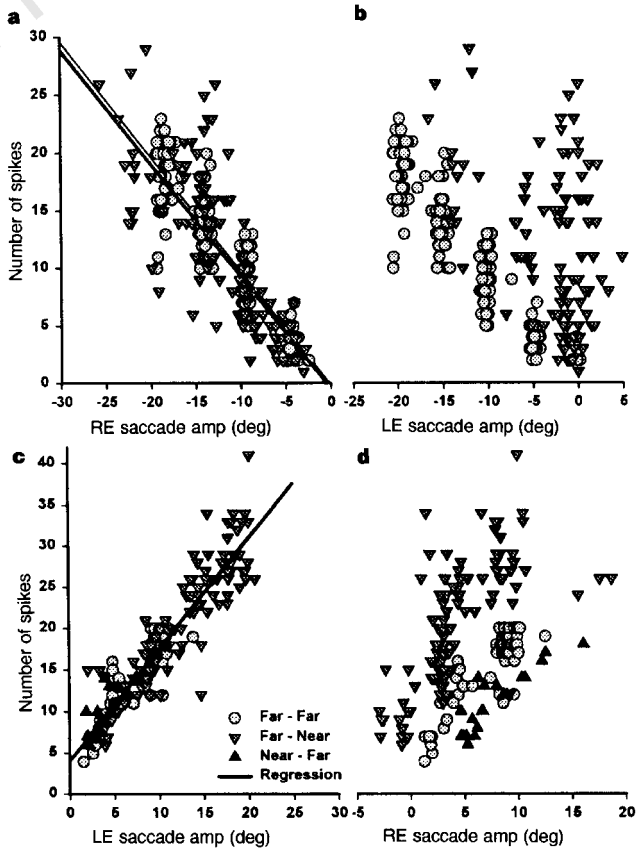

Figure 5 Examples of monocular discharge patterns of 2 EBNs. The number of spikes emitted is proportional to the amplitude of either the right eye saccade (**a**) but not of the left eye saccade (**b**) during disjunctive eye movements. For the other cell, the number of spikes is proportional to the amplitude of the left eye saccade (**c**) but not the right eye saccade (**d**). Both cells discharged if the preferred eye moved toward the recording site and were silent if it moved in other directions. Circles indicate data from conjugate saccade trials; inverted triangles indicate data from convergence saccade trials; and upright triangles indicate data from divergence trials. The thin line (**a**) is the regression for the conjugate data (grey circles); the thick lines (**a**, **c**) are the regressions for all of the data.

Finally, if these cells encode conjugate eye movement, then the regression coefficients for right and left eye should be identical. This was not true for any monocular EBN ($P > 0.05$). To illustrate the distribution of eye preference in the EBN population, we calculated an index of burst ocular selectivity, which is similar to eye position ocular selectivity. Monocular EBNs have ocular selectivities near ± 1 (Fig. 3b, lower panel, black bars). In contrast to motor neurons, however, monocular EBNs were evenly distributed in eye preference (37 ipsilateral and 37 contralateral).

We also recorded 65 NPH neurons that encoded eye position. Like EBNs but in contrast to motor neurons, 78% of the NPH cells were monocular, most of them related to the ipsilateral eye. The most parsimonious interpretation of the predominance of monocular units in the PPRF and NPH is that premotor neurons encode commands for monocular eye movements.

These data indicate a new and quite unexpected organization of a motor system: motor neurons that innervate a single eye may exhibit activity related to movements of either eye, whereas premotor cells, predicted according to Hering's law to encode signals related to movements of both eyes, actually exhibit activity related to movements of one eye. Thus, the basic organization of the oculomotor system is probably monocular, and may be related to an evolutionary inheritance of lateral eyes that move independently. The existence of binocular motor neurons, however, indicates that convergence of premotor monocular signals may be crucial for binocular coordination. The distribution of ocular selectivities in the motor neuron pool may also provide a target for adaptation of ocular alignment, with important consequences for the aetiology and management of abnormal eye alignment (strabismus)[11]. □

Methods

We trained three macaque monkeys to binocularly track a visible target (a laser spot) whose position was controlled by mirror galvanometers. Movements of the left and right eyes were dissociated by aligning the target with one eye and then moving it towards (convergence trials) or away from (divergence trials) the monkey. We assessed the relationship between firing rate and eye movement quantitatively, using multiple regression. Multiple regression analyses were done using a four- (motor neurons and NPH cells) or two- (EBNs) variable linear model: for motor neurons, firing rate was related to the position and speed of the left and right eyes; for EBNs, the number of spikes during the burst was related to the amplitude of left and right eye saccades. For the purpose of brevity, only the data relating to eye position or saccade amplitude are reported here. Eye movements were recorded binocularly using an electromagnetic search coil technique. Animals were prepared for chronic microelectrode recording. We obtained abducens nerve recordings from VIth nerve rootlets ventral to the abducens nucleus and we verified these recordings by microstimulation. EBNs were recorded ventral and rostral to the abducens nucleus.

Received 7 August 1997; accepted 27 March 1998.

1. Helmholtz, J. A. *Treatise on Physiological Optics* (Dover, New York, 1910).
2. Hering, E. *The Theory of Binocular Vision* (Plenum, New York, 1977).
3. Henn, V., Hepp, K. & Büttner-Ennever, J. A. The primate oculomotor system II. Premotor system. *Hum. Neurobiol.* **1,** 87–95 (1982).
4. Henn, V. & Cohen, B. Quantitative analysis of activity in eye muscle motoneurons during saccadic eye movements and positions of fixation. *J. Neurophysiol.* **36,** 115–126 (1973).
5. Henn, V. & Cohen, B. Coding of information about rapid eye movements in the pontine reticular formation of alert monkeys. *Brain Res.* **108,** 307–325 (1976).
6. Luschei, E. S. & Fuchs, A. F. Activity of brainstem neurons during eye movements of alert monkeys. *J. Neurophysiol.* **35,** 445–461 (1972).
7. Fuchs, A. F. & Luschei, E. S. Firing patterns of abducens neurons of alert monkeys in relationship to horizontal eye movement. *J. Neurophysiol.* **33,** 382–392 (1970).
8. Mays, L. E. & Porter, J. D. Neural control of vergence eye movements: activity of abducens and oculomotor neurons. *J. Neurophysiol.* **52,** 743–761 (1984).
9. Fuchs, A. F., Kaneko, C. R. S. & Scudder, C. A. Brainstem control of saccadic eye movements. *Annu. Rev. Neurosci.* **8,** 307–337 (1985).
10. Keller, E. L. Participation of medial pontine reticular formation in eye movement generation in monkey. *J. Neurophysiol.* **37,** 316–332 (1974).
11. King, W. M. & Zhou, W. An ocular selectivity model of eye movement control: implications for strabismus. *Soc. Neurosci. Abstr.* **23,** 1559 (1997).

Acknowledgements. We thank J. Cai for writing the data acquisition software; C. Drake for care of our animals; B.-F. Tang and J. Alison for technical support; and M. Goldberg and P. May for comments on a preliminary version of this manuscript. This research was supported by NIH and ONR grants to W.M.K.

Correspondence and requests for materials should be addressed to W.Z. (e-mail: wuz@vor.umsmed. edu).

Silent glutamatergic synapses and nociception in mammalian spinal cord

Ping Li & Min Zhuo

Department of Anesthesiology, Campus Box 8054, Department of Anatomy and Neurobiology, Washington University in St Louis, St Louis, Missouri 63110, USA

Neurons in the superficial dorsal horn of the spinal cord are important for conveying sensory information from the periphery to the central nervous system[1,2]. Some synapses between primary afferent fibres and spinal dorsal horn neurons may be inefficient or silent[3]. Ineffective sensory transmission could result from a small postsynaptic current that fails to depolarize the cell to threshold for an action potential or from a cell with a normal postsynaptic current but an increased threshold for action potentials. Here we show that some cells in the superficial dorsal horn of the lumbar spinal cord have silent synapses: they do not respond unless the holding potential is moved from −70 mV to +40 mV. Serotonin (5-hydroxytryptamine, 5-HT), an important neurotransmitter of the raphe–spinal projecting pathway, transforms silent glutamatergic synapses into functional ones. Therefore, transformation of silent glutamatergic synapses may serve as a cellular mechanism for central plasticity in the spinal cord.

Silent glutamatergic synapses have been reported in various regions of the central nervous system (CNS)[4–9]. Glutamate is a major fast neurotransmitter in the superficial dorsal horn of the spinal cord[10–12]. We recorded currents from sensory neurons in the superficial dorsal horn of spinal cord slices using whole-cell patch-clamp techniques to test for the existence of silent glutamatergic

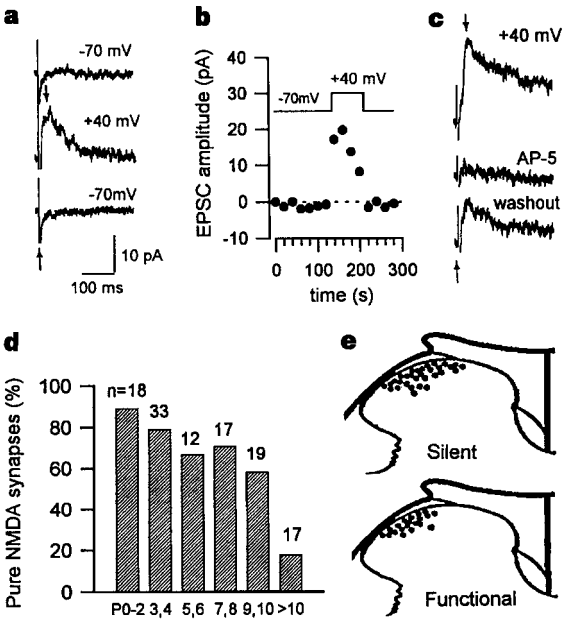

Figure 1 Silent glutamatergic synapses in the lumbar spinal cord. **a**, Examples of responses (the average of three continuous traces) at −70 or +40 mV holding potential. **b**, Time course of the experiment shown in **a**. **c**, Responses at +40 mV were inhibited by 50 μM AP-5. Upward arrow indicates the time of stimulation. Downward arrow indicates the peak currents measured. **d**, The percentage of silent synapses in the superficial dorsal horn of the lumbar spinal cord at P2–17. The numbers of cells tested are indicated above the bars. **e**, Distribution of labelled spinal neurons[28].